Journal of Hazardous Materials 188 (2011) 375–383

Contents lists available at ScienceDirect

Journal of Hazardous Materials

journal homepage: www.elsevier.com/locate/jhazmat

Atmospheric dispersion and individual exposure of hazardous materials

G.C. Efthimiou*, J.G. Bartzis

University of West Macedonia, Department of Mechanical Engineering, Sialvera & Bakola Str., West Macedonia, 50100 Kozani, Greece

ARTICLE INFO

Article history:
Received 15 October 2010
Received in revised form 27 January 2011
Accepted 30 January 2011
Available online 4 February 2011

Keywords:
CFD modeling
Concentration fluctuations
Individual exposure
Turbulent time scales

ABSTRACT

In this work a new approach for CFD RANS modelling of dispersion of airborne point source releases is presented. The key feature of this approach is the model capability to predict concentration time scales that are functions not only of the flow turbulence scales but also of the pollutant travel time. This approach has been implemented for the calculation of the concentration fluctuation dissipation time scale and the maximum individual exposure at short time intervals. For the estimation of travel time in the Eulerian grid the new 'radioactive tracer method' is introduced. The new approaches were incorporated in the CFD code ADREA. The capabilities of the new approaches are validated against the Mock Urban Setting Trial field experiment data under neutral conditions. The comparisons of model and observations gave quite satisfactory results.

1. Introduction

One of the key problems in coping with deliberate or accidental atmospheric releases of hazardous materials is the ability to reliably predict not only the concentration levels but also the maximum individual dosage for a given time interval [1]. This is justified by the fact that the health effects are dependent not only on the magnitude of the pollutant concentration, but also on the duration that the individual is exposed to the high concentration. Therefore, for the assessment of health effects, it is more appropriate to use the dosage, defined as the integral of the concentration over the time interval under consideration. Furthermore due to the stochastic nature of turbulence, the actual concentration, and therefore the actual dosage, at a particular sensor downstream of the source are unknown. The actual dosage at this sensor is expected to lie within a certain range the top of which is termed as the maximum expected dosage. Therefore it is more realistic to utilize the maximum expected dosage rather than the actual one.

The usual methodology to predict the maximum expected concentration/dosage is of probabilistic nature and uses prescribed concentration probability density functions (PDFs) and confidence limits [1]. On the other hand the peak concentration values are expected to be finite [2]. This property in connection with the fact that the probabilistic results are very sensitive to the selected confidence limits, makes the deterministic models more attractive than the probabilistic ones.

Recently, Bartzis et al. [1] have inaugurated an approach relating individual maximum dosage during a time interval $\Delta\tau$ to parameters such as concentration variance and the turbulence integral time scale i.e.

$$D_{\max}(\Delta\tau) = \bar{C}\left[1 + bI\left(\frac{\Delta\tau}{T_c}\right)^{-n}\right]\Delta\tau \quad (1)$$

$D_{\max}(\Delta\tau)$ is the peak dosage, $\bar{C}$ is the mean concentration, b and n are constants that can be estimated experimentally, I is the turbulent fluctuating intensity and T_c is the autocorrelation integral time scale of concentration:

$$I = \frac{\sigma_c^2}{\bar{C}^2}, \quad \sigma_c^2 = \overline{C'^2} \quad \text{and} \quad T_c = \int_0^\infty R(\tau)d\tau \quad (2)$$

where $R(\tau)$ is the concentration autocorrelation function and $\overline{C'^2}$ is the concentration variance.

The need for the estimation of such parameters poses new challenges to modelling capabilities. On the other hand the fact that such releases can happen in complex urban environments poses further difficulties to the whole modelling methodology. For terrains of high complexity it is common to use CFD (Computational Fluid Dynamics) models either LES (Large Eddy Simulation) or RANS (Reynolds Averaged Navier-Stokes) that can treat complex geometries in a more straightforward way. For practical problems the selection of a RANS model in many cases can be the desirable approach since the computer requirements for such models are much less compared to LES models.

CFD RANS models have been widely utilized in the past to estimate mean concentrations from point sources in complex terrains (e.g. [3–5]). The turbulence closure in most of those models is based on the concept of eddy viscosity/diffusivity.

* Corresponding author. Tel.: +30 2461056127; fax: +30 2461021730.
E-mail addresses: gefthimiou@uowm.gr, efthimiougeorgece@gmail.com (G.C. Efthimiou).

0304-3894/$ – see front matter © 2011 Elsevier B.V. All rights reserved.
doi:10.1016/j.jhazmat.2011.01.120

In RANS modelling using the viscosity/diffusivity approach, the transport equation of the mean concentration is usually expressed as follows:

$$\frac{\partial}{\partial t}(\rho\bar{C}) + \frac{\partial}{\partial x_i}(\rho\overline{u_i}\bar{C}) = \frac{\partial}{\partial x_i}\left[\rho(D + K_{ci})\frac{\partial\bar{C}}{\partial x_i}\right] + Q_c \quad (3)$$

where $\overline{u_i}$ are the mean velocity components, D is the molecular diffusivity of the pollutant, $\bar{C}$ is the mean concentration and Q_c is the pollutant sources/sinks.

In the most advanced models – the so called two equation models – the eddy diffusivity vector K_{ci} is simplified to a scalar K_c and is approximated by relations of the type:

$$K_c \propto k^m \xi^n \quad (4)$$

where k is the turbulent kinetic energy and ξ is another turbulent parameter directly or indirectly related to turbulent length scale and/or k. Both parameters are computed from the relevant transport equations. The exponents m and n are derived from non-dimensional analysis.

In the standard two equation turbulent model the parameter ξ is defined as the turbulence energy dissipation ε (e.g. [6]).

Concerning atmospheric flows the standard $k-\varepsilon$ model has been applied successfully in a number of local scale problems such as street canyons, flows over buildings etc. (e.g. [7–9]). However in flows where the domain of interest exceeds the atmospheric surface sublayer, this model proved to be not appropriate without modifications (e.g. [10–14]). Therefore Bartzis [15] has proposed the $k-\zeta$ model which can be implemented to the whole boundary layer [15,16]. The parameter ζ stands for the turbulence integral wavenumber (i.e. the inverse length scale). This new model is able to perform satisfactorily in the whole atmospheric layer. More details of the model are given in [15].

In $k-\zeta$ the eddy diffusivity is given by the relationship:

$$K_c = \frac{1}{\sigma_c} c_\mu k^{1/2} \zeta^{-1} \quad (5)$$

where σ_c is the Schmidt turbulent number equal to 0.74 for neutral conditions. The constant c_μ is equal to 0.1887 as has been calculated in Bartzis [17] from the near wall one-dimensional flow. This same value has been used in the present simulations.

Concerning the concentration fluctuations, in the recent years attempts have been made to estimate the concentration variance by utilizing CFD RANS methodologies (e.g. [18,19]). The typical formulation of the relevant transport equation is as follows:

$$\frac{\partial}{\partial t}(\rho\overline{C'^2}) + \frac{\partial}{\partial x_i}(\rho\overline{u_i}\overline{C'^2}) = 2\rho K_{ci}\left(\frac{\partial\bar{C}}{\partial x_i}\right)^2 + \frac{\partial}{\partial x_i}\left[\rho(D + K_{ci})\frac{\partial\overline{C'^2}}{\partial x_i}\right] - 2\rho D\overline{\frac{\partial C'}{\partial x_i}\frac{\partial C'}{\partial x_i}} \quad (6)$$

where C' is the concentration fluctuation and $\overline{C'^2}$ is the concentration variance.

Concerning the last term in Eq. (6), which is the dissipation rate of concentration variance, the usual modelling approach is to correlate it with the concentration variance and a dissipation time scale T_{dc} [20]:

$$D\overline{\frac{\partial C'}{\partial x_i}\frac{\partial C'}{\partial x_i}} = \frac{\overline{C'^2}}{T_{dc}} \quad (7)$$

A considerable amount of work exists in the literature concerning the modelling of T_{dc} (e.g. [9,18–20]). In the two equation models T_{dc} is usually scaled by the relevant turbulent parameterization applying dimensional analysis. In the study of Efthimiou et al. [21] the turbulent modelling approach for T_{dc} using the $k-\zeta$ turbulence model was expressed as:

$$T_{dc} = c_{dc}\, k^{-1/2} \zeta^{-1} \quad (8)$$

The constant c_{dc} is equal to 3.05 as has been calculated in Efthimiou et al. [21] from sensitivity simulations of the MUST experiment. This value has been used in the present simulations.

The above mentioned CFD RANS methodology creates some question about the model reliability near the source. Taylor [22] has already pointed out that turbulent diffusion differs in the near and the far regions from a continuous point source. In the proximity of the source, fluid particles retain the memory of their initial turbulent environment [23]. For long travel times, this memory is lost, and particles follow mainly the local properties of turbulence [24]. From a theoretical point of view the concentration turbulence parameterization in general is always affected by the travel time of pollutant especially near the source (e.g. [23,25–28]). On the other hand, according to the author's current knowledge based in the open literature, the travel time effect on the concentration turbulence parameterization has not been taken into consideration on the complex Eulerian CFD modelling. The innovation of the present study is to introduce in such models the effect of the travel time in the turbulence time scales T_c and T_{dc}. It is noticed that in the present work the whole model validation has been restricted to neutral atmospheric conditions.

2. The present methodology

In the present methodology the transport Eqs. (3) and (6) are considered valid predicting the mean concentration and the concentration variance field respectively. The individual maximum exposure is given by Eq. (1).

Following Bartzis [15] the turbulence closure is based on the eddy viscosity concept and the two equation $k-\zeta$ model.

The overall approach has been incorporated to ADREA code [29]. ADREA is a three dimensional RANS CFD code. The turbulence closure modelling is limited for now to eddy viscosity/diffusivity concept. Anisotropic effects are also included. Zero, one and two-equation schemes are available. ADREA utilizes a finite volume methodology for the numerical solution of the conservation equations, with a staggered grid for the velocities. It is fully implicit in time while it uses second order scheme for the convective terms. The SIMPLER/ADREA algorithm is adopted, which consists of transforming the mixture mass conservation equation into a full pressure equation, overall solution per time step by an iterative procedure, solution per variable by the various numerical methods including Biconjugate Gradient Stabilized Method [30] and automatic time step selection based on convergence error bands. The equations are solved on a Cartesian, non equidistant grid.

2.1. The time scales

Let us assume stationary turbulence and the von Karman distribution for the frequency spectrum of the wind speed u [31]:

$$\frac{n\, S_u(n)}{\sigma_u^2} = \frac{0.58 n T_0}{[1 + 1.49(n\, T_0)^2]^{5/6}} \quad (9)$$

where $S_u(n)$ is the power spectrum of u and σ_u^2 is its variance.

T_0 is the 'resonance' time scale i.e. the time scale corresponding to the frequency of the peak spectral value.

Experimental evidence has shown that for well mixed conditions the velocity's and concentration's frequency power spectra profiles have the same form [32]. In this case the autocorrelation integral time scale of concentration (T_c) can be represented by T_u.

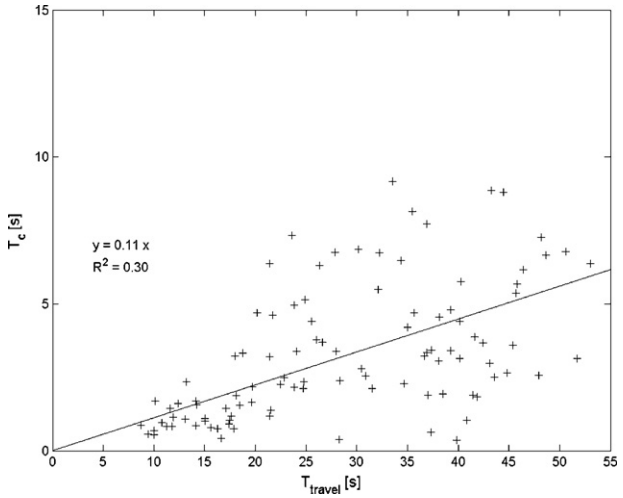

Fig. 1. Derivation of the parameter c_u for Eq. (12). Axis x is the pollutant travel time as has been estimated by ADREA code and axis y is the experimental autocorrelation integral time scale of concentration (trials MUST T-11, T-12).

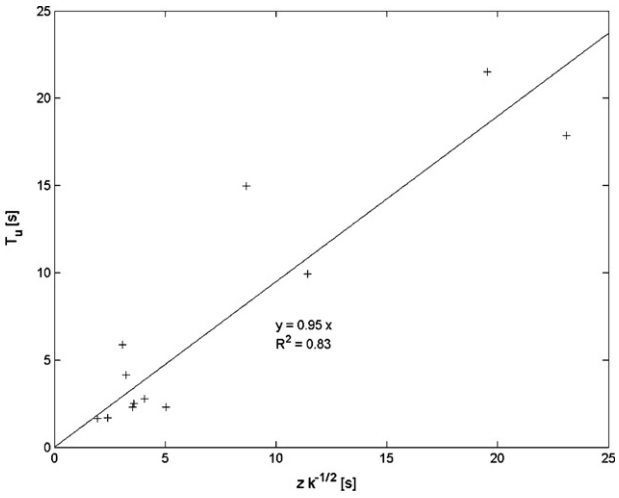

Fig. 2. Derivation of the parameter c_h for Eq. (14). Axis x is the model $zk^{-1/2}$ and axis y is the experimental autocorrelation integral time scale of velocity (trials MUST T-11, T-12).

It can be proved that T_u is linearly related with the resonance time scale T_0 [33]:

$$T_u = 0.146\, T_0 \tag{10}$$

Based on the abovementioned discussion, it is reasonable to assume that when the receptor is getting very close to the source, the resonance time scale to be dominated by the pollutant travel time (T_{travel}) i.e.

$$T_0 \approx T_{\text{travel}} \tag{11}$$

If this is the case one has to examine whether a relationship analogous to Eq. (10) is valid:

$$T_c \approx c_u\, T_{\text{travel}} \tag{12}$$

and that the analogy constant c_u is of the order of magnitude of the theoretical one (0.146).

In order to prove the validity of Eq. (12) and to have a first estimate at the same time of the proportionality constant c_u the data of the MUST (Mock Urban Setting Trial) field experiment has been exploited [34,35]. The MUST is an experiment in real field, flat terrain, with a regular array of 120 obstacles (will be described analytically in Section 3). The relevant dataset includes two trials (T11 and T12) corresponding to neutral atmospheric conditions and contains high resolution concentration time series ($\Delta\tau = 0.01$–0.02 s) from 72 sensor measurements for each trial. Fig. 1 shows the experimental T_c (estimated by Eq. (2)) versus the pollutant travel time T_{travel} (estimated by the ADREA code as will be described in Section 2.2) for the above mentioned sensors. Despite the data scattering a linear correlation between T_c and T_{travel} is clear with c_u value equal to 0.11. The linearity of the data and as a result the validity of Eq. (12) is supported also from the fact that the parameter b from the general formula of the straight line $y = ax + b$ was found to be very close to zero (=0.34), with a proportionality constant a equal to 0.1 and a nearly same correlation coefficient $R^2 \approx 0.3$. The implementation of the same fit ($y = ax + b$) to every trial of MUST separately gives the parameter b close to zero and the constant a close to c_u with an uncertainty ±2%. For this uncertainty of the constant c_u the sensitivity studies that performed have shown negligible differences on the results.

It was interesting to find out that the experimental c_u value is close to the theoretical one (=0.146) a fact that clearly supports the validity of the assumption (11). It is noticed that for more precise values further experimental evidence is needed. It should be added here that the T_{travel} dominance over T_0 in each individual sensor is difficult to check and this could explain the relatively high scattering of the data.

These results and the previous discussion allow us to propose the following simple relationship – as a first order approximation – for the autocorrelation time scale of concentration:

$$T_c = \min(c_u\ T_{\text{travel}}, T_u) \tag{13}$$

Based on the above analysis the proposed value of c_u is the one obtained from the experiments i.e. $c_u = 0.11$.

T_u is the hydrodynamic autocorrelation time scale, which in the current work is derived by applying $k - \zeta$ parameterization i.e.

$$T_u = c_h k^{-1/2} \zeta^{-1} \tag{14}$$

The value of c_h constant is also expected to be derived from experimental evidence. It has been estimated from the present MUST hydrodynamic data for both trials. In Fig. 2 the experimental T_u is plotted against the parameter $zk^{-1/2}$. The data considered, refer to sensors that are well within the atmospheric surface (maximum height 16 m) layer and sufficiently far from the ground obstacles (minimum height 4 m). In this case it is expected $\zeta \approx 1/z$. Fig. 2 shows the strong correlation of T_u with the vertical distance z as expected. The linear best-fit suggests $c_h = 0.95$. Due to the small number of data in Fig. 2, the authors considered that it was important to perform a sensitivity study for the constant c_h by using values based on the 95% confidence bounds of the prediction of c_h (from a lower bound 0.8 to a higher bound 1.2) and negligible differences in the results have been observed. The same sensitivity study for this parameter had been performed also in the simulations of the paper [16] and the same conclusions were drawn. So for modelling purposes the selection of values of $c_h \approx 0.8$–1.2 is generally acceptable. In this study c_h was set equal to 1.0 in the middle of this range. It is noticed that for more precise values further experimental evidence is needed.

Concerning the dissipation time scale utilized in Eq. (8) it is plausible to scale it with the autocorrelation time scale T_c i.e.

$$T_{dc} = c_d T_c \tag{15}$$

The value of the constant c_d for the well mixed conditions can be derived from Eqs. (8) and (14):

$$c_d = 3.05 \tag{16}$$

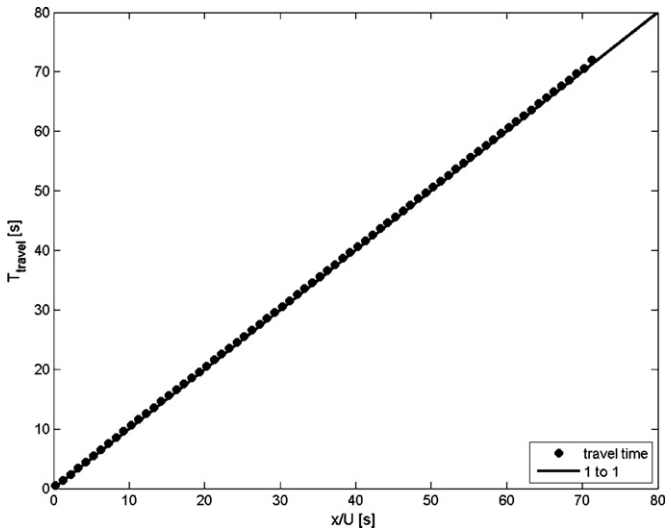

Fig. 3. Comparison of the pollutant travel time between the physical law x/U and Eq. (18) along the plume centerline.

2.2. The travel time

The travel time in Eulerian models is not straightforward. In this work a new method is introduced to estimate pollutant travel time, the so called 'radioactive tracer method'. Two passive tracers are released simultaneously from the same pollutant source with the same release rate conditions equal to the experimental one. The tracers are released from the same source in order to ensure that the travel time is exactly the same for both tracers. One of the tracers is inert whereas the other one is considered 'radioactive' with a decay constant λ [s^{-1}]. For the radioactive pollutant the source term Q_c in Eq. (3) is given as follows:

$$Q_c = -\lambda C \tag{17}$$

In a receptor point the concentration of the radioactive tracer is expected to be lower than the concentration of the inert tracer. The difference is due to the fact that the radioactive tracer experiences a decay due to radioactivity directly dependent on the time passed between its generation time in the source and its arrival time at the receptor. In mathematical terms, let C_0 and C be the concentrations of the inert and radioactive tracer respectively. The travel time then is given by the relationship $C/C_0 = e^{-\lambda T_{\text{travel}}}$ or:

$$T_{\text{travel}} = -\frac{1}{\lambda}\ln\frac{C}{C_0} \tag{18}$$

The concentrations C and C_0 are obtained by solving the respective transport equations of type (3) for the two tracers. It is noticed that in general, the concentration in a particular sensor is built by pollutant material coming from various paths (especially in wake regions) with different travel times. The value in Eq. (18) represents an average value of these travel times.

A validation of this methodology has been attempted in an ideal problem of a point source in an infinite medium with uniform velocity U and constant diffusivity K_c. For such a problem the travel time at the plume centerline is equal to x/U: where x is the distance from the source along the centerline.

For the numerical simulation of the problem the following reasonable values are selected for the input parameters: $U = 5\ \text{ms}^{-1}$, $K_c = 5\ \text{m}^2\ \text{s}^{-1}$ and $Q_{\text{source}} = 1\ \text{m}^3\ \text{s}^{-1}$.

The source height is taken arbitrarily at 7.5 m above the ground. The decay constant was set equal to $1 \times 10^{-4}\ \text{s}^{-1}$. The calculations have been obtained by $88 \times 88 \times 38$ grid with uniform grid size in lateral directions $dx = dy = 5$ m and in vertical direction $dz = 1$ m.

Table 1
MUST experimental characteristics of the selected trials.

Experiment	Trial 11 (200 s)	Trial 12 (200 s)
Tracer	Propylene (C_3H_6)	
Configuration	Complex terrain	
Release duration	15 min	
Release rate (Q_{source})	0.00457 kg s^{-1}	
Source area	0.00196 m^2	
Ambient temperature	≈31 °C	
Surface roughness	0.045 m	
Average wind speed (V_h)	7.93 m s^{-1} (at 4 m height)	7.26 m s^{-1} (at 4 m height)

The results are presented in Fig. 3. It is obvious that the present method predicts perfectly the travel time along the centerline which is a strong indication of its validity.

3. The present validation studies

In the present work Trials 11 and 12 of the MUST field experiment [34,35] have been considered for model validation due to the fact that they correspond to neutral conditions. The experimental characteristics of these trials are given in Table 1.

The MUST experiment, Trials 11 and 12, is a well established experiment with high quality concentration and meteorological measurements. The MUST experiment took place at the Horizontal Grid on the U.S. Army Dugway Proving Ground, located in the Great Basin Desert of northwestern Utah during September 2001 [34,35]. A total of 120 standard size shipping containers were set up in a nearly regular array consisting of 12 rows of 10 obstacles, covering an area of around 200 by 200 m. Each obstacle was a standard shipping container of width 12.2 m, length 2.42 m, and height 2.54 m. At a position near the center of the container array, a so-called VIP van was used, serving as collection point for sampled wind and concentration data. The size of the VIP van differs significantly from the size of the surrounding conex containers. A schematic diagram of the MUST array as well as the locations of the concentration instruments can be found in Yee and Biltoft [35]. Tracer gas was measured from 48 fast-response photoionization detectors (DPIDs) and 24 Ultraviolet Ion Collectors (UVICs). In this study for both trials a period of 200 s from the concentration time series was selected for the calculation of concentration statistics corresponding to neutral conditions. This period was originally chosen by Yee and Biltoft [35] and was primarily based on the stationarity (i.e. speed and direction) of the wind over the period.

3.1. The MUST simulations and results

3.1.1. The numerical simulations

In Fig. 4, the computational domain for the Trials T11 and T12 MUST simulations is presented. The total size of the domain was 274 m in the streamwise direction (x), 299 m in the spanwise direction (y) and 32 m in the vertical direction (z).

The discretization of the computational domain was $170 \times 99 \times 44$ hexahedral cells. The minimum/maximum sizes of the discretization cells along x-, y- and z-directions were taken 1.2/6.48 m, 2.5/6.59 m and 0.32/1.57 m respectively.

The simulations were performed in two steps. In the first step the one-dimensional equations in the vertical direction were solved in order to obtain the vertical profiles of velocity, turbulent kinetic energy and wavenumber ζ. The selected incident wind direction was nearly −41° for both trials, relative to the x-axis, and as a result the equations for both the u and v velocity components had to be solved. The computational grid consisted of 267 grid points (first cell-centre distance from the ground ≈0.159 m) and extended up to nearly 4000 m. The ground surface was treated as rough wall,

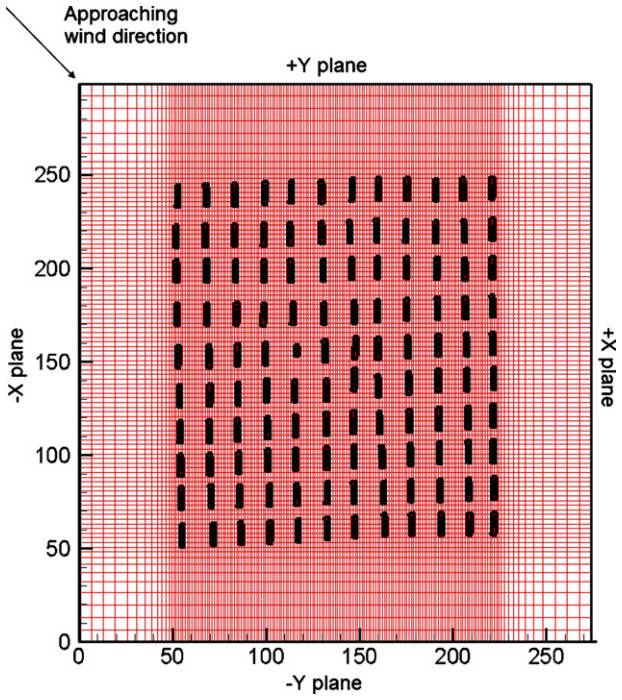

Fig. 4. The computational domain of the MUST T-11 and T-12 simulations.

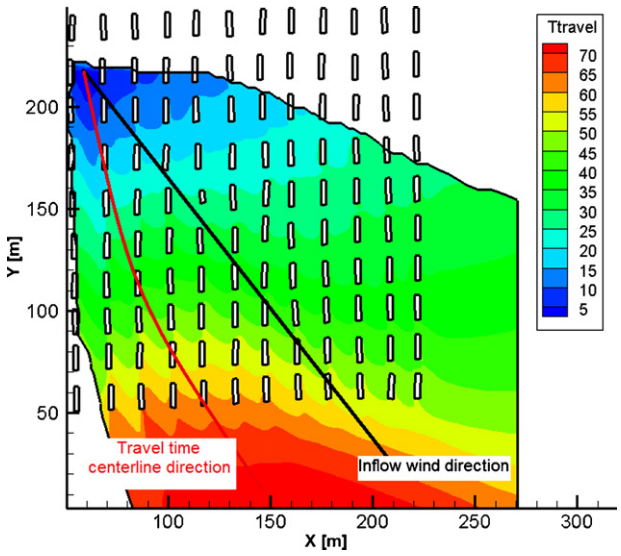

Fig. 5. Horizontal plane of the pollutant travel time at the height of 1.8 m for trial MUST-T12, showing the evolution of the travel time away from the source as well as the deflection of the travel time centerline direction (red line) from the inflow wind direction (black line). (For interpretation of the references to color in this figure legend, the reader is referred to the web version of the article.)

using the standard wall functions with the experimental roughness length $z_0 = 0.045$ m. At the top of the domain (4000 m) the geostrophic wind components U_g and V_g were given as input to the model and their selection was made in order to obtain the velocities u and v in agreement with the experimental ones at particular measurement heights. Also the Coriolis parameter f was used as input for the calculations based on the latitude of the MUST experiment (Utah, USA).

In the second computational step the full three-dimensional flow and dispersion calculations were performed using as initial and boundary conditions the profiles obtained from the first step up to the height of 32 m. These vertical profiles were kept constant at the two inlet lateral planes of the domain i.e. the $-x$ and $+y$ planes (Fig. 4). At the other two lateral planes of the domain ($+x$ and $-y$ planes), outlet boundary conditions were imposed. The $-z$ plane (ground surface) was treated as rough wall with the same roughness length ($z_0 = 0.045$ m). The buildings were treated as rough walls with a very small roughness length ($z_0 = 10e-05$ m). At the top of the domain, symmetry boundary conditions were used. Concerning the pollutant source, it has been modeled by an irregular surface that has been placed inside the computational domain at the same location and height with the experiment. The area of the surface, the release rate and the physical properties of the actual pollutant (propylene) were the same as for the experiment (Table 1). The second computational step was treated as a true transient state problem. The total calculation time was selected as large as possible in order for the pollutants to cross the entire computational domain.

The calculated three-dimensional fields of pollutant mean, variance and maximum mass fractions were first transformed to ppm to be comparable with the experimental data. Subsequently they were interpolated to obtain the values at the exact locations of the DPID and UVIC measurements. All model results and experimental measurements have been normalized according to the following equation:

$$C^* = \frac{CV_hH^2}{Q_{\text{source}}} \tag{19}$$

where C is the computed or measured concentration in ppm, V_h is the mean horizontal speed at the 4 m level of the upwind mast, H is the height of the containers equal to 2.54 m and Q_{source} is the release rate of propylene (Table 1).

3.1.2. Travel times

In Fig. 5 the 2D field of the travel time model is presented for Trial 12 on an horizontal plane at the height of the source 1.8 m. It is obvious that the evolution of the travel time is logical away from the source i.e. lower near the source and greater far downstream. Also it is interesting to observe how the particular building arrangement deflects the travel time centerline (red line) relative to the inflow wind direction axis (black line, -41.2°) as expected.

3.1.3. Mean concentrations

Fig. 6a and b displays the scatter plot for the mean arc-maximum concentrations for Trial 11 and Trial 12 representing two well defined neutral cases. In this study the arc-maximum is defined as the maximum observed value of a sensor among sensors that line up on the same horizontal line (see Fig. 1 in Yee and Biltoft [35] for the arrangement of the four horizontal lines). The comparison between the observations and the predictions is performed for these particular sensors. It is noticed that the maximum arc concentrations are of main concern in exposure assessment. For both trials the results are very good and all lie within a factor of two of observations, an ideal fact for field experiment validation comparisons. The concentration at the first sensor nearest to the source is slightly overestimated. This tendency is reversed for the lower values, which are closer to the 1:1 line.

Also in order to evaluate the total performance of the mean concentration model, validation metrics have been used. These are the fractional bias (FB), the normalized mean square error (NMSE) and the factor of two of observations (FAC2) [36]. It should be noted that for the calculation of these metrics only pairs for which the observed measurements were non-zero have been selected. The results for the mean concentration validation metrics of Trial 11 and Trial 12 are presented in Table 2. The sensor results have been grouped in two sets. For each trial the first set consists of 30 sensors that were placed near the ground on an array of four horizontal lines [34,35], where the human exposure is more direct. The sec-

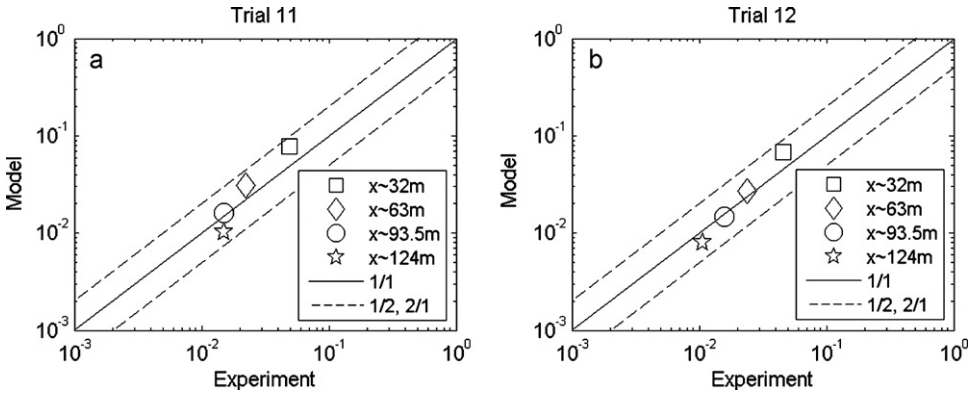

Fig. 6. Comparison of the mean arc-maximum concentrations between MUST observations and ADREA predictions on four monitoring arcs (32 m, 63 m, 93.5 m and 124 m) for (a) Trial 11 and (b) Trial 12.

ond set consists of 52 sensors and contains the first set (30 sensors) and 22 sensors that were placed on vertical towers. The second set gives the model overall performance.

Concerning the model performance with regards to metrics, the COST 732 guidelines [36] require the following quality acceptance criteria: FAC2 > 50%, |FB| < 0.3 and NMSE < 4 for mean concentrations. It should be noticed also that normally someone expects the field predictions to be worse than the wind tunnel predictions because the hydrodynamic and turbulent field in a wind tunnel is better defined especially in terms of inlet and boundary conditions.

In case of Trial 11, the FAC2 is relatively high for the near ground measurements (60%), indicating that the model predicts well the observed mean concentrations. Also the FB and the NMSE values (−0.08 and 0.35 respectively) indicate that the model gives a small over-prediction and scatter of the observations respectively. Overall all the metrics for the near ground measurements fulfil well the quality acceptance criteria. Concerning the total measurements, it is obvious that the FAC2 is slightly below the limit (48% < 50%), while acceptable values for the NMSE (0.69) and the FB (−0.24) have been calculated.

In case of Trial 12, the results are very good both for the near ground measurements and the total measurements. It is worth to notice that for the near ground measurements the FAC2 is equal to 89% which is a very good result for a field experiment validation study. The scatter is similar to Trial 11 (NMSE = 0.33) while the FB value (−0.22) indicates that the model over-predict more the observations than Trial 11. Totally for all the measurements the model predicts very well the observations (FAC2 = 70%) with a small scatter in the data (NMSE = 0.42) and a small over-prediction (FB = −0.19). Overall all the metrics of Trial 12 fulfil the quality acceptance criteria.

At this point it should be noted that for both trials the lower FAC2 of the total measurements comparing with the one of the ground measurements suggests that in the elevated sensors the results show larger discrepancies. Preliminary sensitivity studies have shown that one important factor for such discrepancies seems to be the absence of input vertical wind into the model. The data

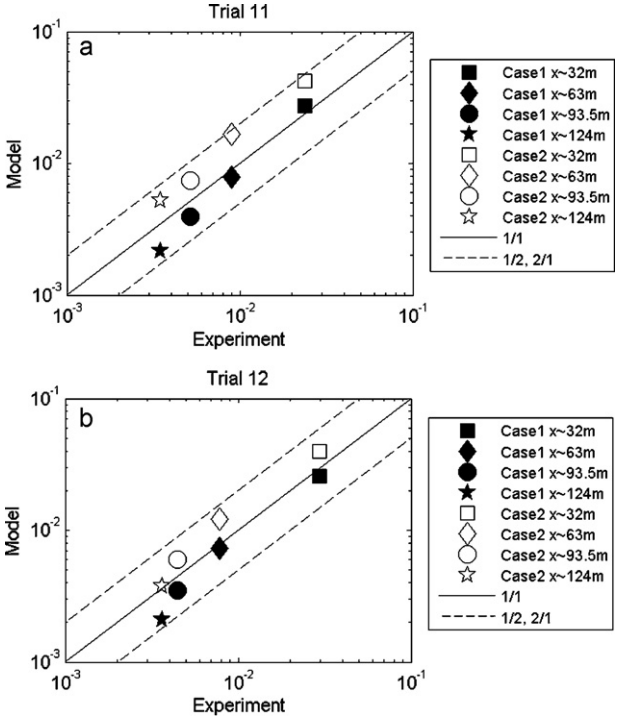

Fig. 7. Comparison of the arc-maximum concentration standard deviation between MUST observations and ADREA predictions (Case 1, Case 2) on four monitoring arcs (32 m, 63 m, 93.5 m and 124 m) for (a) Trial 11 and (b) Trial 12.

Table 2
Validation metrics for the mean concentration of trial MUST-T11 and MUST-T12. The results have been grouped in near ground measurements and total measurements.

MUST T-11	Near ground measurements	Total
FAC2	0.60	0.48
NMSE	0.35	0.69
FB	−0.08	−0.24
MUST T-12	Near ground measurements	Total
FAC2	0.89	0.70
NMSE	0.33	0.42
FB	−0.22	−0.19

Table 3
Validation metrics for the concentration standard deviation of trials MUST-T11 and MUST T-12. The results have been grouped in near ground measurements and total measurements.

Near ground measurements			
	FB	NMSE	FAC2
Trial 11 (Case1/Case2)	0.21/−0.41	0.22/1.23	0.63/0.60
Trial 12 (Case1/Case2)	0.075/−0.30	0.088/0.35	0.82/0.67
Total			
	FB	NMSE	FAC2
Trial 11 (Case1/Case2)	−0.33/−1.11	1.39/7.63	0.59/0.38
Trial 12 (Case1/Case2)	−0.35/−0.933	1.20/4.71	0.76/0.48

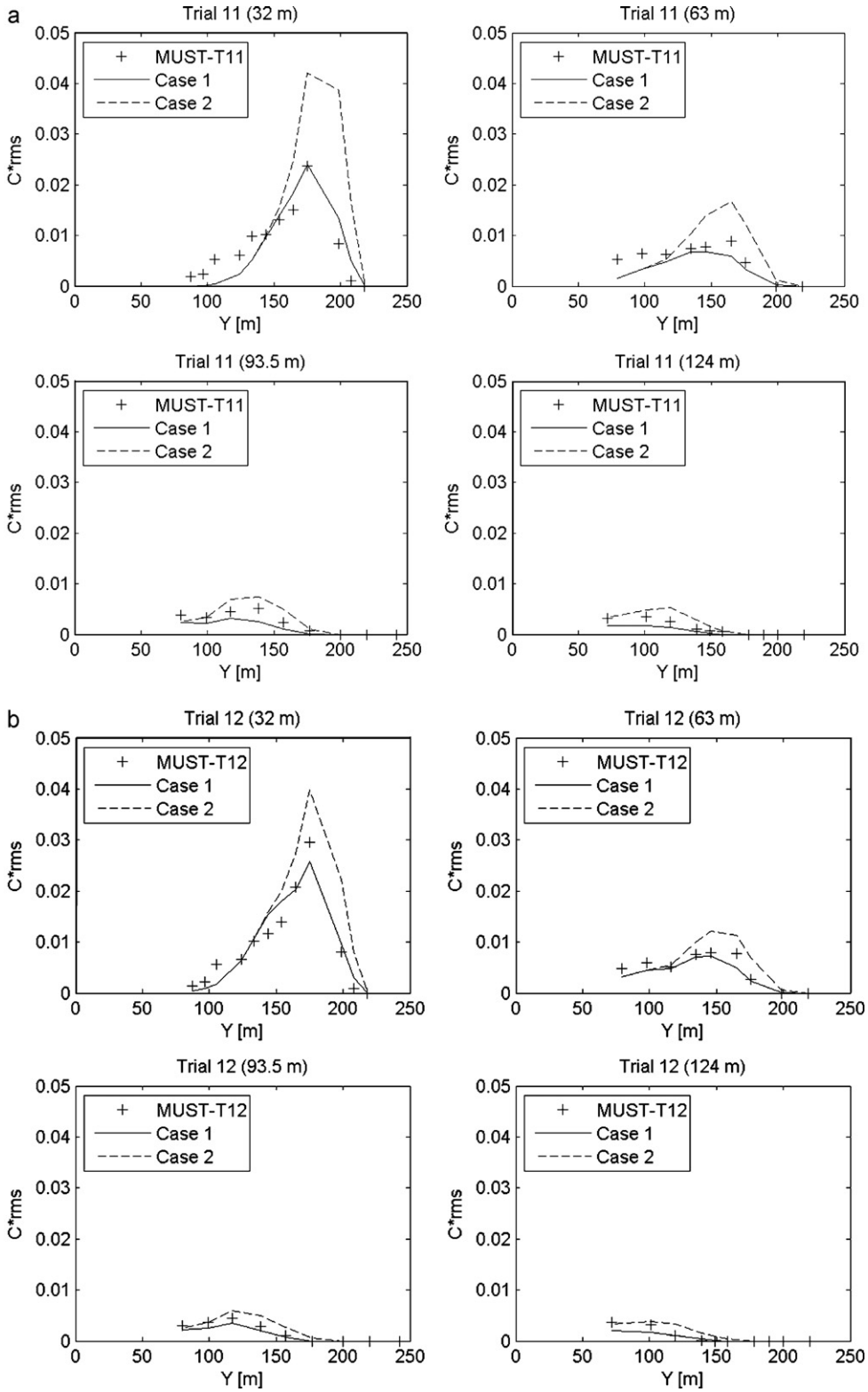

Fig. 8. Horizontal profiles of the concentration standard deviation of MUST observations and ADREA predictions (Case 1, Case 2) on four horizontal lines (32 m, 63 m, 93.5 m and 124 m) for (a) Trial 11 and (b) Trial 12.

were not enough to provide large scale vertical wind input to the present local scale model. Vertical winds seem to be a likely cause for the trend presented in Fig. 6 i.e. from average concentration overestimation at the shortest distance from release point to underestimation at the largest distance. A detailed analysis of the data has not presented any sensitivity/effect from the pollutant inlet model.

As a conclusion for the mean concentration, the model predicts very well the observations especially for the near ground measurements where the human exposure is more direct.

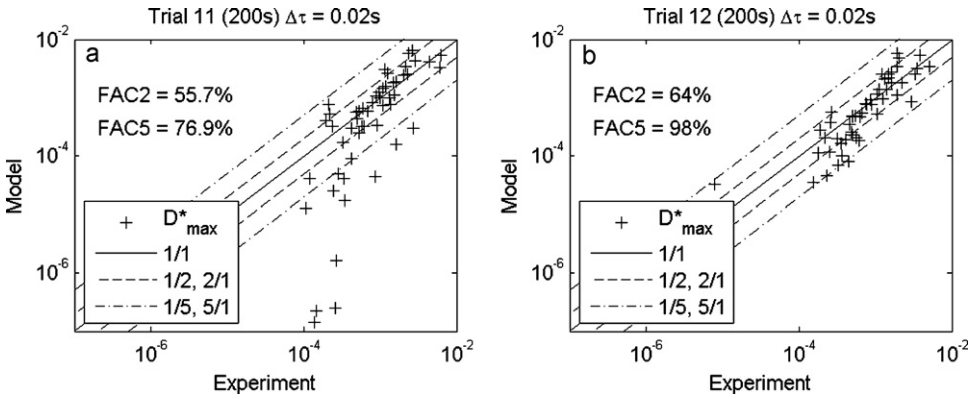

Fig. 9. Comparison of peak dosages ($\Delta\tau = 0.02$ s) for (a) Trial 11 and (b) Trial 12. The modeled peak dosages have been estimated utilizing Eq. (7) as obtained by the present model (Case 1).

3.1.4. Concentration standard deviation

For the model validation purposes, two computational cases have been performed as follows:

Case 1: The concentration time scale T_c depends on the pollutant travel time (Eq. (13)).
Case 2: The time scales are pollutant travel time independent and well mixed conditions are assumed.

Fig. 7a and b displays the scatter plots for the arc-maximum concentration standard deviation for both trials. From the figures it is obvious that Case 1 shows better performance than Case 2 near the source as expected.

This ascertainment is strengthened also by Fig. 8a and b which displays the horizontal profiles of the concentration standard deviation for both trials. From the figures it is clear that at the first and the second horizontal lines which are closest to the source the predictions of the travel time dependent model are in better agreement with the observations than the corresponding independent one.

The validation metrics for the concentration standard deviation are presented in Table 3. The results have been grouped in a similar way as the mean concentration results (i.e. near ground and total measurements). The number of data for each group is the same as the mean concentration. In this point it should be noticed that there are no guidelines that specify quality acceptance criteria for the metrics of the concentration standard deviation. Due to the fact that the fluctuations exhibited in the time series of measured concentrations are often at least of the same order of magnitude as the mean concentration, the same state-of-art values can be used to validate the model. For the near ground measurements it is obvious that the FAC2 of Cases 1 and 2 is comparable for Trial 11 (63.3% and 60% respectively), while Case 1 presents a higher FAC2 for Trial 12 (82%) than Case 2 (67%). Also the FB values (Trial 11: 0.21, Trial 12: 0.075) indicate that Case 1 underpredicts the near ground measurements and this was also obvious in Fig. 8. Case 1 gives lower values for the NMSE than Case 2 indicating a smaller scatter in the data. Totally for all the measurements Case 1 predicts better the observations than Case 2 as expected by giving higher values for the FAC2 and smaller values for the NMSE and the FB. It is obvious also that the metrics of Case 1 fulfil the quality acceptance criteria for all measurements, except the FB of the total measurements which is slightly higher than the limit (Trial 11: 0.33, Trial 12: 0.35, limit: 0.3).

As a conclusion for the concentration standard deviation, the travel time dependent model shows in general better behaviour than the corresponding travel time independent one especially near the source. The lower predicted values of Case 1 compared to Case 2 is based on the fact that the travel time dependent dissipation time scale causes a higher decay of concentration standard deviation near the source. This has a local as well as downstream effect due to convection. Vertical winds are also an important factor for the trend presented in Fig. 7 as has been explained also in Section 3.1.3.

3.1.5. Individual exposure

Modeled peak dosages have been estimated for the time interval $\Delta\tau = 0.02$ s (the time resolution for most of the measurements) utilizing Eq. (1) as obtained by the present model (Case 1). The experimental values have been derived by selecting the peak value

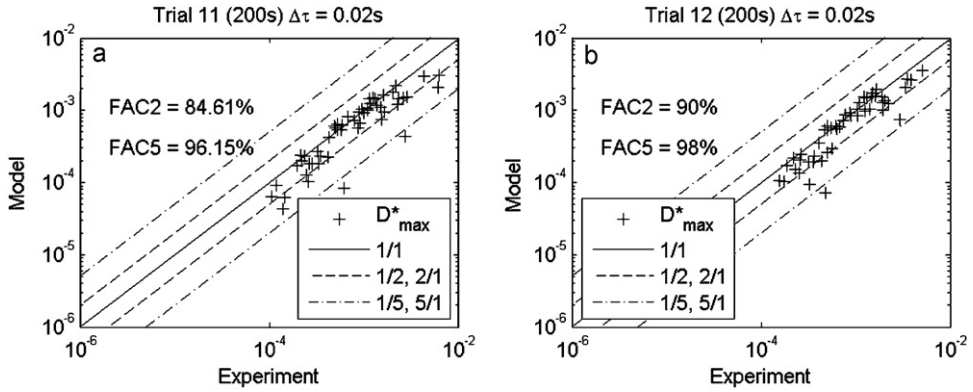

Fig. 10. Comparison of peak dosages ($\Delta\tau = 0.02$ s) for (a) Trial 11 and (b) Trial 12. The modeled peak dosages have been estimated by applying Eq. (7) using the experimental concentration mean and variance while the time integral scale has been obtained by the model.

from the concentration time series integrals over time increments $\Delta\tau$. The results for both trials are shown in Fig. 9.

Both trials have very good FAC2 (Trial 11: 55.7%, Trial 12: 64%) and FAC5 (factor of five of observations) (Trial 11: 76.9%, Trial 12: 98%). The discrepancies for both trials seem to come mainly from the errors in estimating the concentration mean and variance. This becomes more clear in Fig. 10. In this case the modeled peak dosages have been estimated by applying Eq. (1) using the experimental concentration mean and variance while the time integral scale has been obtained by the model. In this case all the predicted dosages are nearly inside the factor of two of observations (Trial 11: 84.61%, Trial 12: 90%) supporting further the validity of Bartzis et al. [1] model to predict peak dosages within a factor of two.

4. Conclusions

A new approach is introduced in air dispersion modelling from point sources utilizing CFD RANS modelling able to predict not only mean concentration but also concentration variance and individual exposure in short time intervals.

The key elements of this approach is:

- The new model for autocorrelation and dissipation turbulent time scales prediction (Eqs. (14) and (15)).
- The dependence of concentration time scales on pollutant travel time in the near source region (Eq. (13)).
- The estimation of pollutant travel time based on the so called 'radioactive tracer method' (Eq. (18)).

Two trials in neutral conditions from the MUST experiment (complex terrain) [34,35] have been considered for model validation.

The present model gives in general good results especially for the near ground measurements where the human exposure is more direct. In fact the calculated validation metrics of the present model fulfil well the COST 732 quality assurance criteria.

The predictions of the concentration standard deviation are better in case of the travel time dependent model than the corresponding independent one especially near the source where the travel time effect is stronger.

Finally, the implementation of the empirical model Bartzis et al. [1] into the present RANS CFD model to estimate short time maximum exposure gives satisfactory results strengthening further the validity of this model.

It should be noted that the 'radioactive tracer method' has been implemented successfully for the MUST case, which is considered as moderately complex terrain. Applications of the present methodology in more complex urban configurations need to be studied in the future.

Acknowledgements

The authors would like to thank the Defense Threat Reduction Agency (DTRA) and COST Action 732 providing access to the MUST data.

References

[1] J.G. Bartzis, A. Sfetsos, S. Andronopoulos, On the individual exposure from airborne hazardous releases: the effect of atmospheric turbulence, J. Hazard. Mater. 150 (2008) 76–82.
[2] J.G. Bartzis, G.C. Efthimiou, Maximum individual exposure estimation using CFD RANS modelling, in: Proceedings of the 13th International Conference on Harmonization within Atmospheric Dispersion Modelling for Regulatory Purposes, Paris, France, 2010, pp. 858–862.
[3] M. Milliez, B. Carissimo, Numerical simulations of pollutant dispersion in an idealized urban area for different meteorological conditions, Boundary-Layer Meteorol. 122 (2007) 321–342.
[4] J.L. Santiago, A. Martilli, F. Martin, CFD simulation of airflow over a regular array of cubes. Part I: three-dimensional simulation of the flow and validation with wind tunnel measurements, Boundary-Layer Meteorol. 122 (2007) 609–634.
[5] R.P. Donelly, T.J. Lyons, T. Flassak, Evaluation of results of a numerical simulation of dispersion in an idealized urban area for emergency response modelling, Atmos. Environ. 43 (2009) 4416–4423.
[6] B.E. Launder, D.B. Spalding, The numerical computation of turbulent flows, Comp. Meth. Appl. Mech. Eng. 3 (1974) 269–289.
[7] J. Baik, J. Kim, A numerical study of flow and pollutant dispersion characteristics in urban street canyons, J. Appl. Meteorol. 38 (1999) 1576–1589.
[8] C.H. Chang, R.N. Meroney, Numerical and physical modeling of bluff body flow and dispersion in urban street canyons, J. Wind Eng. Ind. Aerodyn. 89 (2001) 1325–1334.
[9] K.J. Hsieh, F.S. Lien, E. Yee, Numerical modeling of passive scalar dispersion in an urban canopy layer, J. Wind Eng. Ind. Aerodyn. 95 (2007) 1611–1636.
[10] H.W. Detering, D. Etling, Application of the E–e turbulence model to the atmospheric boundary layer, Boundary-Layer Meteorol. 33 (1985) 113–133.
[11] P.G. Duynkerke, Application of the E–$\in$ turbulence closure model to the neutral and stable atmospheric boundary layer, J. Atmos. Sci. 45 (1988) 865–880.
[12] A. Andren, C.H. Moeng, Single point closures in a neutrally stratified boundary layer, J. Atmos. Sci. 50 (1993) 3366–3379.
[13] D.D. Apsley, I.P. Castro, A limited-length scale k–e model for the neutral and stably-stratified atmospheric boundary layer, Boundary-Layer Meteorol. 83 (1997) 75–98.
[14] D. Xu, P.A. Taylor, An E–e–l turbulence closure scheme for planetary boundary layer models: the neutrally stratified case, Boundary-Layer Meteorol. 84 (1997) 247–266.
[15] J.G. Bartzis, New approaches in two-equation turbulence modelling for atmospheric applications, Boundary-Layer Meteorol. 116 (3) (2005) 445–459.
[16] G.C. Efthimiou, J.G. Bartzis, N. Koutsourakis, Modelling concentration fluctuations and individual exposure in complex urban environments, J. Wind Eng. Ind. Aerodyn. (2011), doi:10.1016/j.jweia.2010.12.007.
[17] J.G. Bartzis, Turbulent diffusion modelling for wind flow and dispersion analysis, Atmos. Environ. 23 (1989) 1963–1969.
[18] S. Andronopoulos, D. Grigoriadis, A. Robins, A. Venetsanos, S. Rafailidis, J.G. Bartzis, Three-dimensional modelling of concentration fluctuations in complicated geometry, Environ. Fluid Mech. 1 (2002) 415–440.
[19] M. Milliez, B. Carissimo, Computational fluid dynamical modeling of concentration fluctuations in an idealized urban urea, Boundary-Layer Meteorol. 127 (2008) 241–259.
[20] G.T. Csanady, Concentration fluctuations in turbulent diffusion, J. Atmos. Sci. 24 (1967) 21–28.
[21] G. Efthimiou, J. Bartzis, S. Andronopoulos, A. Sfetsos, Air dispersion modelling for individual exposure studies, J. Environ. Pollut. submitted for publication.
[22] G.I. Taylor, Diffusion by continuous movements, Proc. Lond. Math. Soc. 20 (1921) 196–212.
[23] K.S.M. Essa, M. Embaby, New formulations of eddy diffusivity for solution of diffusion equation in a convective boundary layer, Atmos. Res. 85 (2007) 77–83.
[24] G.K. Batchelor, Diffusion in a field of homogeneous turbulence, Eulerian analysis, Aust. J. Sci. Res. 2 (1949) 437–450.
[25] J. Neumann, Some observations on the simple exponential function as a Lagrangian velocity correlation function in turbulent diffusion, Atmos. Environ. 12 (1978) 1965–1968.
[26] H. Tennekes, The exponential Lagrangian correlation function and turbulent diffusion in the inertial subrange, Atmos. Environ. 12 (1979) 1565–1567.
[27] J.H. Seinfeld, S.N. Pandis, Atmospheric Chemistry and Physics: From Air Pollution to Climate Change, John Wiley & Sons Inc, NewYork, USA, 1998.
[28] A.G. Goulart, D.M. Moreira, J.C. Carvalho, T. Tirabassi, Derivation of eddy diffusivities from an unsteady turbulence spectrum, Atmos. Environ. 38 (2004) 6121–6124.
[29] J.G. Bartzis, A. Venetsanos, M. Varvayani, N. Catsaros, A. Megaritou, ADREA-I: a three-dimensional transient transport code for complex terrain and other applications, Nucl. Technol. 94 (1991) 135–148.
[30] H.A. Van der Vorst, Bi-CGSTAB: a fast and smoothly converging variant of Bi-CG for the solution of nonsymmetric linear systems, SIAM J. Sci. Stat. Comput. 13 (1992) 631–644.
[31] C.W. Park, S.J. Lee, The effects of bottom gap and non-uniform porosity in a wind fence on the surface pressure of a triangular prism located behind the fence, J. Wind Eng. Ind. Aerodynam. 89 (2001) 1137–1154.
[32] K.R. Mylne, P.J. Mason, Concentration fluctuation measurements in a dispersing plume at a range of up to 1000 m, Q. J. Roy. Met. Soc. 117 (1991) 177–206.
[33] T. von Karman, Progress in the statistical theory of turbulence, Proc. Natl. Acad. Sci. 34 (1948) 530–539.
[34] C.A. Biltoft, Customer report for Mock Urban Setting Test, DPG Document No. WDTC-FR-01-121, West Desert Test Center, U.S. Army Dugway Proving Ground, Dugway, Utah, (2001).
[35] E. Yee, C.A. Biltoft, Concentration fluctuation measurements in a plume dispersing through a regular array of obstacles, Boundary Layer Meteorol. 111 (2004) 363–415.
[36] M. Schatzmann, H. Olesen, J. Franke, COST 732 Model Evaluation Case Studies: Approach and Results, COST Office, 2009, http://www.mi.uni-hamburg.de/Official-Documents.5849.0.html.